**Stem Cell Reports, Volume *5***

**Supplemental Information**

# Cell Division Mode Change Mediates the Regulation of Cerebellar Granule Neurogenesis Controlled by the Sonic Hedgehog Signaling

**Rong Yang, Minglei Wang, Jia Wang, Xingxu Huang, Ru Yang, and Wei-Qiang Gao**

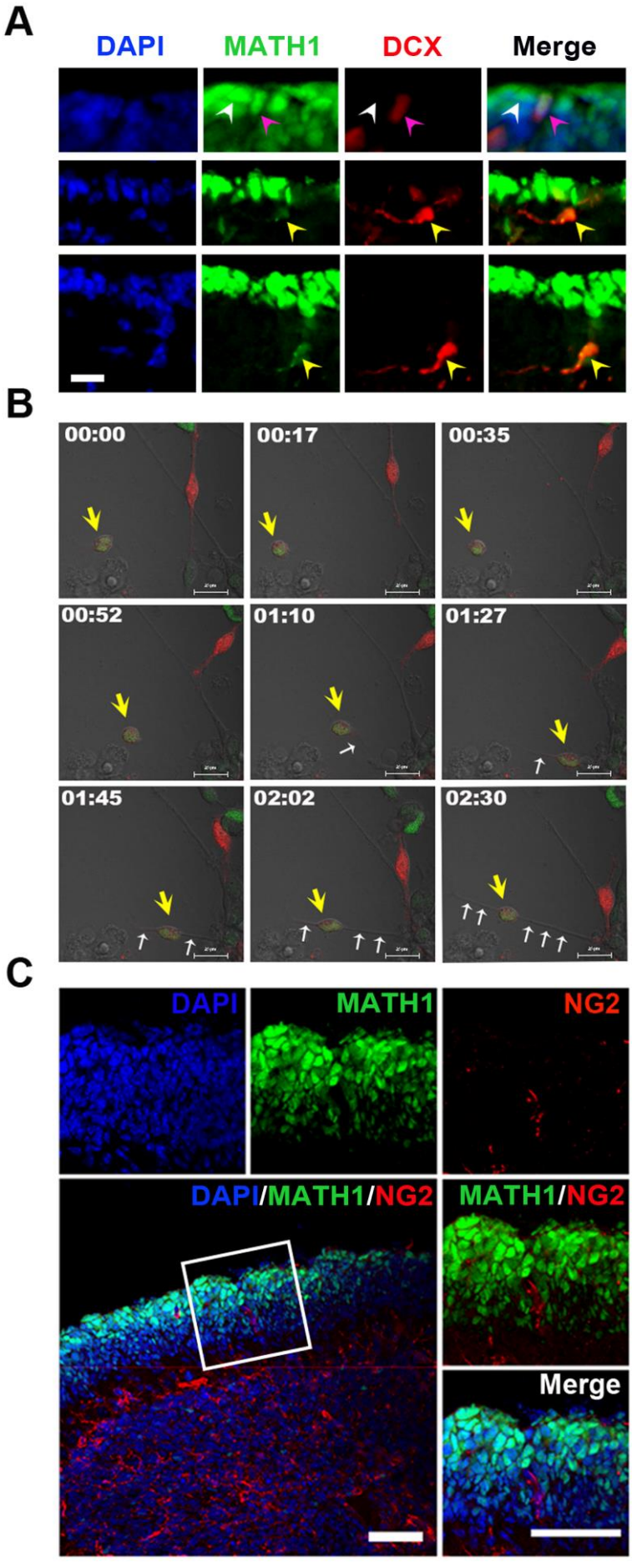
A
DAPI
MATH1
DCX
Merge
B
00:00
00:17
00:35
00:52
01:10
01:27
01:45
02:02
02:30
C
DAPI
MATH1
NG2
DAPI/MATH1/NG2
MATH1/NG2
Merge

**Figure S1. Granule neuronal progenitors (GNPs) look like "epitheloid cells" *in vivo*.** (A) Confocal images of sagittal sections from the *Math1-GFP; Dcx-DsRed* mouse cerebellum at P11. In the upper panel, white arrowheads indicate MATH1-GFP GNPs and purple arrowheads indicate MATH1-GFP/DCX-DSRED double positive intermediate cells without process. In the medium panel, yellow arrowheads indicate MATH1-GFP/ DCX-DSRED double positive intermediate cells with processes in EGL. In the lower panel, yellow arrowheads indicate MATH1-GFP/ DCX-DSRED double positive intermediate cells with processes in the deeper layer of EGL. Scale bars: 10 μm. (B) Nine selected frames from Movie 1, a 2.5-h time-lapse sequence of MATH1-GFP and DCX-DSRED double positive intermediate cells. The images show that neuronal processes (indicated by small white arrows) extended gradually from yellow intermediate cells (indicated by yellow arrows), which change from epitheloid cells to polyhedral cells. Scale bars: 20 μm. (C) Confocal images of sagittal sections from the *Math1-GFP* mouse cerebellum at P9. NG2 (red) was used to stain polyhedral cells. GNPs were not stained by NG2 antibody. Scale bars: 50 μm. See also Movie 1. Figure S1 related to Results.

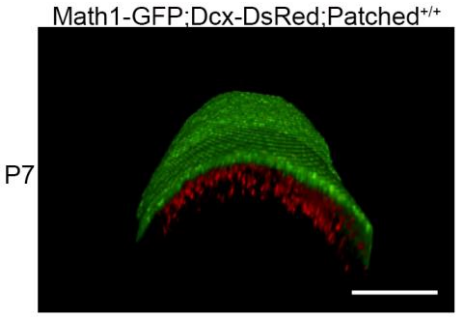


**Figure S2. No intermediate cell is detected in wild type mice at P7.** By performing multi-photon fluorescence microscopy, we examined the three-dimensional (3D) reconstruction of cerebella in freshly dissected whole mount cerebella from *Math1-GFP; Dcx-DsRed; Patched*$^{+/+}$ mouse strain. We did not detect intermediate cells (yellow) in the *Math1-GFP; Dcx-DsRed; Patched*$^{+/+}$ mouse strain at P7 during cerebellar neurogenesis. Scale bars: 100 μm. Figure S2 related to Figure 5.

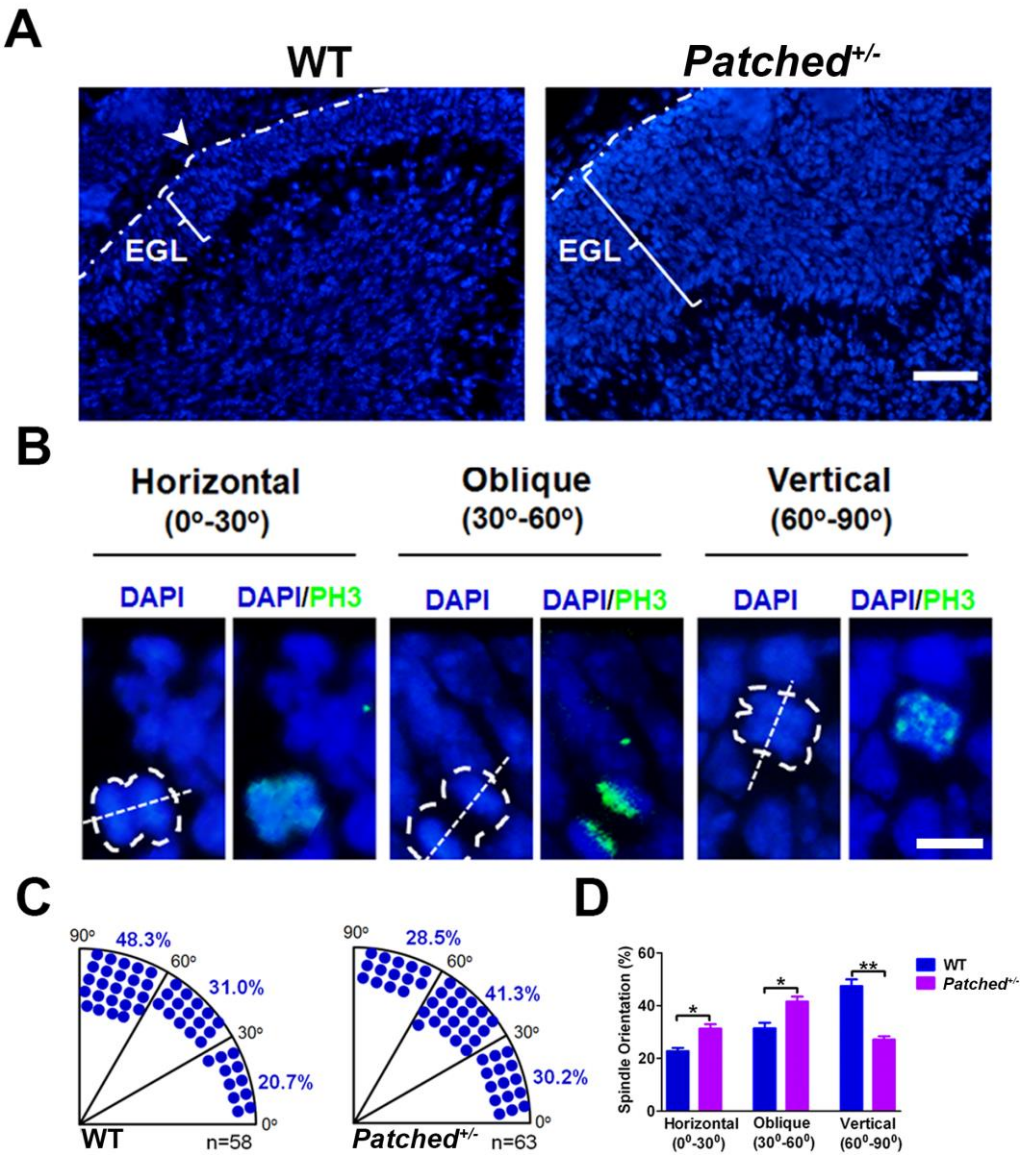


**Figure S3. Activation of SHH signaling can alter spindle orientation of GNPs divisions.** (A) Activation of SHH signaling enhances the thickness of EGL during cerebellum development as reported. The white arrowhead indicates the EGL pial surface. Scale bars: 50 μm. (B) Examples of three different classes of GNPs divisions, horizontal, oblique or vertical to the pial surface of the cerebellum at P11. PH3 (green) marks mitotic DNA and spindle orientations. DAPI (blue) was used as nuclear counterstain. Scale bars: 5 μm. (C and D) Angle distribution of spindle orientation in GNPs from wild type and *Patched*$^{+/-}$ mouse cerebella (C) and statistic analysis of the angles of spindle orientation (D). The data we collected are from 58 dividing cells in wild type mice and from 63 dividing cells in *Patched*$^{+/-}$ mice, which were from 3 independent experiments. Data are shown as mean ± s.e.m.. *P<0.05, ** P<0.01, referring to the numbers of horizontal, oblique or vertical divisions in wild type vs *Patched* mutant mouse cerebella at P11. Figure S3 related to Results.

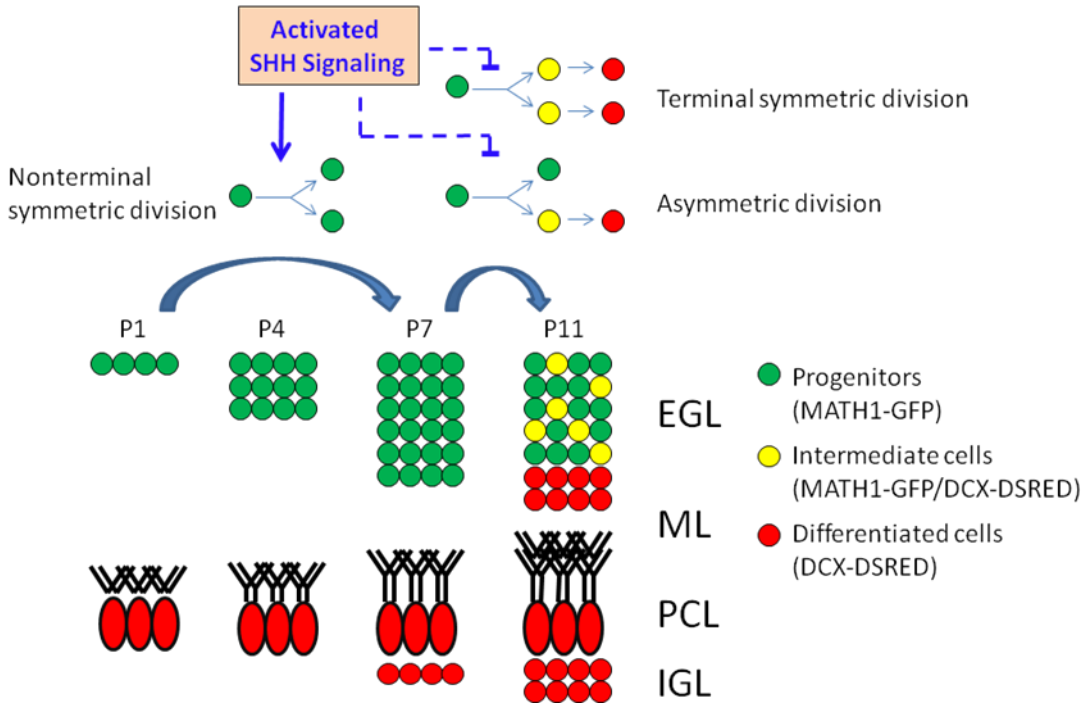


**Figure S4. Cell division modes and SHH signaling in cerebellar neurogenesis.** A model proposed to indicate that the change of non-terminal symmetric, terminal symmetric and asymmetric cell divisions mediates the regulation of cerebellar granule neurogenesis governed by the sonic hedgehog signaling. Figure S4 related to Discussion.

**Movie 1. The morphological change of MATH1-GFP and DCX-DSRED double positive intermediate cells.** A 2.5-h time-lapse sequence of live images for MATH1-GFP and DCX-DSRED double positive intermediate cells shows that neuronal processes (indicated by small white arrows) extend gradually from yellow intermediate cells (indicated by yellow arrows), indicating that MATH1-GFP/ DCX-DSRED double positive intermediate cells are morphologically at the stage of changing from epitheloid cells to polyhedral cells. Movie 1 related to Figure S1.

**Movie 2. Representative symmetric division of granule neuron progenitor cells *in vitro*.** Symmetric division generating two MATH1-GFP daughter progenitors from a MATH1-GFP mother cell was captured by time-lapse recording in cultured granule neuron progenitor cells from *Math1-GFP; Dcx-DsRed* mice (P10). A 1.5-h time-lapse sequence of live image shows that a MATH1-GFP cell on the right (blue arrow) undergoes a symmetrically division. Movie 2 related to Figure 2.

**Movie 3. Representative asymmetric division of granule neuron progenitor cells *in vitro*.** A 1.5-h time-lapse sequence of live images shows that a MATH1-GFP mother cell from *Math1-GFP; Dcx-DsRed* mice (P10) undergoes an asymmetric division, generating one MATH1-GFP progenitor cell (blue arrow) and one intermediate cell (white arrow) which co-expressing MATH1 and DCX. Movie 3 related to Figure 2.

**Movie 4. Representative non-terminal symmetric division of granule neuron progenitor cells *ex vivo*.** A 1.5-h time-lapse sequence of live images for granule neuron progenitor cells shows that a MATH1-GFP cell on the left (blue arrow) undergoes symmetric division, generating two MATH1-GFP progenitors (blue arrow). Movie 4 related to Figure 3.

**Movie 5. Representative asymmetric division of granule neuron progenitor cells *ex vivo*.** A 1-h time-lapse live image recording shows that a MATH1-GFP cell on the left (blue arrow) undergoes an asymmetric division, generating one MATH1-GFP progenitor (blue arrow) and one MATH1 and DCX co-expressing cells (white arrow). Movie 5 related to Figure 3.

**Movie 6. Representative terminal symmetric division of granule neuron progenitor cells *ex vivo*.** A 2-h time-lapse live image recording shows that a MATH1-GFP cell (blue arrow) undergoes terminal symmetric division, generating two DCX-DSRED differentiated cells (red). Movie 6 related to Figure 3.

## Supplemental Experimental Procedures

### Histo-immunofluorescence staining

Cerebella were collected from mice and fixed overnight in 4% paraformaldehyde. After incubated sequentially in PBS buffer with 10% and 30% sucrose, the tissue specimens were frozen in embedding medium (O.C.T compound) and sectioned into 10μm thick slices for immunofluorescent staining.

For immunofluorescence staining, tissue specimens were blocked in PBS with 10% donkey serum or 10% goat serum for 1 hour at RT. After blocking, specimens were incubated overnight with rabbit anti-NG2 (Abcam) at 1:500, and mouse anti-PH3 (Cell Signaling Technology) at 1:500. Following 3 times of washes in PBS, specimens were incubated with secondary antibodies conjugated either with Alexafluor 488 or Alexafluor 594 (Jackson Lab) at a 1:600 dilution for 1 hour.

Coverslips were mounted on a slide using a mounting medium containing DAPI. Slides were stored at $4^0$C and images were taken within one week. Images were acquired with a Leica confocal microscope and analyzed with LCS confocal software (Leica).